Analytical Methods

Accepted Manuscript

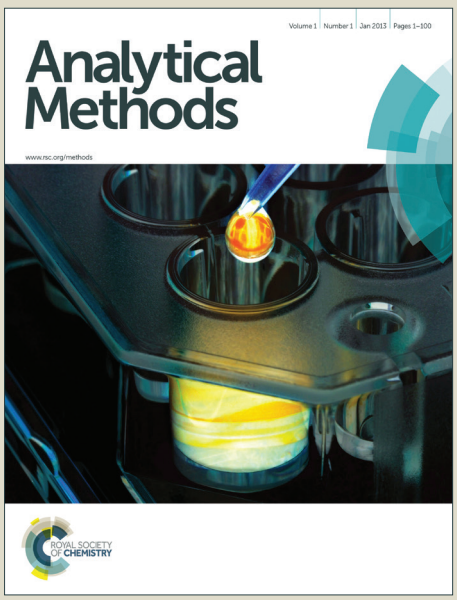

ROYAL SOCIETY OF CHEMISTRY

www.rsc.org/methods

Selective Detection of Organophosphate Nerve Agents using Microplasma Device

Bo Wang, Wenqing Cao, Yixiang Duan *

Research Center of Analytical Instrumentation, College of Chemistry, Sichuan University, Chengdu 610064, P. R. China;

* Address correspondence to: Prof. Yixiang Duan, Research Center of Analytical Instrumentation, Sichuan University, 29 Wangjiang Road, Chengdu, 610064, China.

E-mail: yduan@scu.edu.cn.

Phone: (+86)028-85418180. Fax: (+86)028-85418180.

ABSTRACT

Direct current glow discharge microplasma source permits ambient ionization directly and can provide fast and accurate *in-situ* detection combined with spectrometer. In this study, a stable microplasma-based detector for nerve agent detection has been developed. The innovative concept of this new nerve agent detector is to detect two parts of the nerve agent components, phosphorous element and organic part of CH radicals at the same time. Because there are two detection targets, our microplasma-based detector has enhanced selectivity to nerve agents. The reasons for this characteristic are studied through comparing the emission spectra of the microplasma and microwave plasma. We suggest that it's the very low gas temperature of our microplasma source that makes it possible to excite the nerve agents molecules without decomposition or split of the CH component. Thus the spectrometer can detect the emission lines of phosphorous element and organic part of CH radicals simultaneously. The influence of discharge current and gas flow rate on phosphorus signal intensity has been investigated. The emission intensity of phosphorus at 253.6 nm increases linearly with the discharge current in our tested range, but nonlinearly with the gas flow rate. The detection curve has been calibrated. The emission intensity at 253.6 nm is in proportion to the concentration of the specimen triethyl phosphate (TEP) in the range from 41 ppm to 500 ppm by volume. The detection limit was calculated to be 5 ppm by volume. Small size, low power, low cost, and high selectivity make our device very suitable for nerve agents scanning in the field.

1 Introduction

Nerve agents are a class of phosphorus-containing organic chemicals, organophosphates (OP), which disrupt the mechanism by which nerves transfer messages to organs. They can be categorized into two groups, G-type and V-type. The nerve agents of G-type, GA (tabun, O-Ethyl N, N-dimethyl phosphoramidocyanate), GB (sarin, O-Isopropyl methylphosphonofluoridate), GD (soman, O-Pinacolyl methylphosphonofluoridate), and GF (cyclosarin, O-Cyclohexyl methylphosphonofluoridate) contain typical P-F or P-CN bond. G-type nerve agents are volatile and rapidly hydrolyzing compounds.[1] The two major V-type agents are VX [O-ethyl S-(2-diisopropylaminoethyl) methylthiophosphonate] and R-VX [O-isobutyl S-(2-diethylaminoethyl) methylthiophosphonate]. The chemical structures of the typical nerve agents are shown in Fig. 1. The main hydrolysis pathways of these typical agents have been reviewed by Hooijschuur et al. [1] and Pumera.[2]

Usually, a functioning motor nerve is stimulated and it releases the neurotransmitter acetylcholine (ACh), which transmits the impulse to a muscle or organ. Once the impulse is sent, the enzyme ACh esterase immediately breaks down the ACh in order to allow the muscle or organ to relax. Upon dermal or respiratory contact, nerve agents disrupt the nervous system by inhibiting the enzyme ACh esterase through forming a covalent bond with the site of the enzyme where ACh normally undergoes hydrolysis. Because ACh builds up and continues to act, any nerve impulses are continually transmitted, and muscle contractions do not stop.[3]

Owing to this harmful effect to human beings, nerve agents have become a serious threat to the society, thus studying rapid and reliable methods for the determination of nerve agents and their degradation products is necessary. It's known that chromatography (GC) is the most widely used method for its high efficiency and the possibilities for volatile compounds detection. Since nerve agents are rather volatile compounds with sufficient thermal stability, and, in addition, contain a phosphorus (P) atom, gas chromatography-mass spectrometry (GC–MS)[1], GC with flame photometric detection (FPD) or GC with nitrogen-phosphorus detection (NPD) are very suitable combinations for selective nerve agents detection and quantification[4] and play the major role nowadays. The other techniques include flame ionization detection (FID),[5] photoionization detection (PID),[6] ion mobility spectrometry (IMS),[12] Fourier transform infrared spectroscopy (FTIR),[7–9] semiconducting sensors,[10, 11] and direct air-sampling mass spectrometry[13-18]. However, some of these techniques have their individual limitations for nerve agent detection. GC–MS is complex to operate, difficult to maintain, expensive to build, and time-consuming. Though existing portable GC–MS can provide useful analytical power, GC–MS is not amenable to timely response in the field since it needs significant vacuum to maintain a high vacuum condition. Semicoducting sensors based upon general physical or chemical properties

typically rely upon non-specific detection. They are responsive only to changes in total vapor concentrations and, therefore, are hardly applicable to specific nerve agent detection. IMS has been considered as a potential tool for nerve agent detection. However, the number of IMS instruments deployed as field detectors for real samples is still very limited because the instrument suffers problems of poor selectivity and memory effect. Technologies with mass spectrometry can provide specific and sensitive real-time detection, however the volume of the instruments are too bulk to use on-site.[14] Flame photometry is widely recognized as highly sensitive method for chemical warfare agents detection through burning chemical agents with a hot hydrogen flame and measuring particular spectral lines of phosphorous. However, the method is prone to false-positive results by detecting other gases that contain significant amount of phosphorous such as routine environmental samples like sulfur dioxide and hydrogen sulfide. Due to this limitation, the flame photometry has to be combined with some other separation methods such as gas chromatography, which make the system complex, time-consuming, and impractical for field use.

Nowadays, a novel method, microplasma technology, matches well with the requirements for organic compounds detection, mainly because these techniques allow fast and reliable *in situ* detection by a small size, simple structure microplasma discharge chamber. These microplasmas can be coupled with optical emission spectrometry (OES) or mass spectrometry(MS) for sensitive and selective detection of molecular fragments and even for elemental analysis.[19, 20] Moreover, they are used in ambient conditions and easy to be fabricated. Thus the diminutive volume and the low cost of the apparatus ingratiate them with the demands of rapid scanning of the nerve agents on field.

In this paper, we report a new detector for nerve agent detection through using a microplasma source for sample fragmentation and excitation and measuring elemental/molecular emission spectrum. Our new nerve agent detector is to take the advantages of a small, low temperature, inert gas supported plasma to detect two parts of the nerve agent components, phosphorous element and organic part of CH radicals simultaneously without any preparation and pretreatment, instead of one targeted component (element) in flame photometry. In this way, interferences can be avoided from environmental samples as they usually have no organic components, thus our method can provide more reliable results with less detecting time than flame photometry technique and can be built readily, which make our device suitable for nerve agents scanning *in situ*. Furthermore, the low gas temperature makes our microplasma source more stable since there is no carbon deposition like other plasma-based techniques usually do. The characteristics of the microplasma discharge, the influence of plasma gas flow rates, and discharge voltages are studied. The sensitivity of the

new device is also examined through detecting the detection limits of triethyl phosphate (TEP) which is 5 ppm by volume.

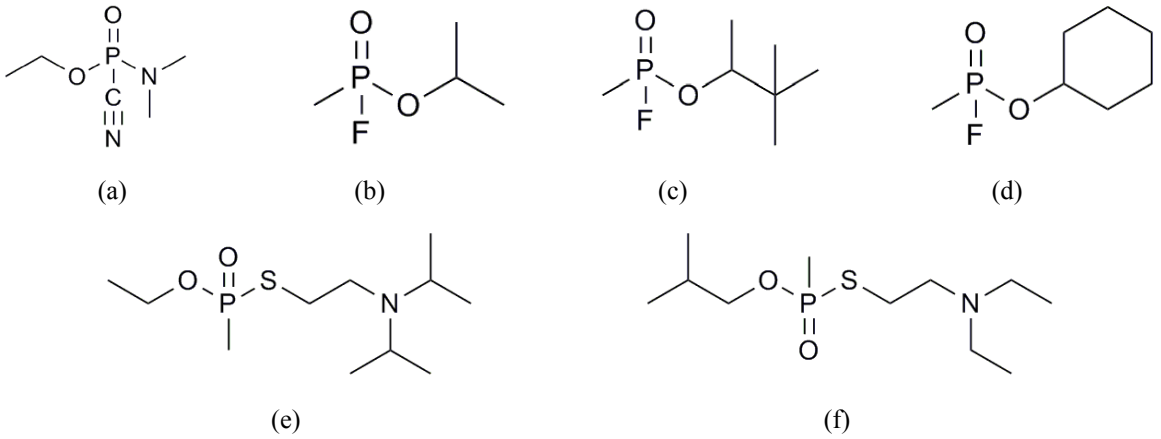

Fig.1 Chemical structures of typical nerve agents: (a) GA (tabun, O-Ethyl N, N-dimethyl phosphoramidocyanate), (b) GB (sarin, O-Isopropyl methylphosphonofluoridate), (c) GD (soman, O-Pinacolyl methylphosphonofluoridate), (d) GF (cyclosarin, O-Cyclohexyl methylphosphonofluoridate), (e) VX [O-ethyl S-(2-diisopropylaminoethyl) methylthiophosphonate], and (f) R-VX [O-isobutyl S-(2-diethylaminoethyl) methylthiophosphonate].

2 Experimental methods

2.1 Reagents and gases

In view of the safety issue, a nerve agent stimulant, triethyl phosphate (TEP) (99%), was used in this study. TEP is the triester of ethanol and phosphoric acid and can be called “phosphoric acid, triethyl ester”. The formula and chemical structure of TEP is shown in Fig. 2. An ultra-high purity argon gas (99.999%, provided by QiaoYuan Gas Company, China) (traditionally > 99% is feasible) was used in two channels to carry the sample into the discharge chamber as sample gas and generate microplasma as carrier gas.

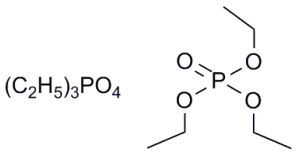

Fig.2 Formula and chemical structure of triethyl phosphate (TEP).

2.2 Microplasma generator

The construction of microplasma device has been described in our previous paper.[22] Briefly, two platinum plate electrodes were bonded to two 96% Alumina substrates, where the two electrodes were placed face to

face to construct a discharge chamber. The discharge chamber measured 500 μm height × 500 μm width × 600 μm depth (150nL). A DC voltage was applied to the electrodes for atmospheric pressure plasma generation in argon. To compare the analytical ability with another kind of plasma based technology, a microwave plasma was introduced. The microwave plasma was built up by a 100W microwave power with frequency of 2.45 GHz which was coupled into an adjustable cylindrical copper resonant cavity. A hollow glass tube with a 3 mm inside diameter and 5 mm outside diameter threaded though the resonant cavity along the axis of the cylindrical resonant cavity. Plasma was generated with argon as well.

2.3 Measurement system

A schematic drawing of the detection system using atmospheric pressure microplasma is shown in Fig. 3. The mass flow rates (MFR) in sample and carrier gas channels were adjusted through two FC-260 Mass Flow Controllers (Tylan Corporation, US), which were electronically controlled via a 5878 4-channel power supply/readout unit. Carrier gas and sample gas channels were fed with ultra-high purity argon. Generally speaking, He can generate plasma as well, however to combine the plasma with spectrometer, Ar with longer flame was the better choice than He, of which the flame was difficult to flow out the chamber. The argon in sample channel flowed through a sealed flask containing TEP. A magnetic stirrer was employed to stir TEP in the sealed flask. With adequate stir and a suitable sample gas flow rate at 233.5 mL min^{-1}, the TEP vapor in the flask was assumed saturated. As shown in Figure 3, the saturated TEP vapor was diluted by argon with the dilution rate 0.99 and then introduced into the discharge chamber. With a suitable carrier gas flow rate at 1000 mL/min and DC voltage at 280V applied to the two discharge electrodes, a microplasma was generated at atmospheric pressure. A collimate lens was used to collect the light emitted from the plasma chamber and focus the beam into an optical fiber. The optical emission was guided to an Ocean Optics USB2000 spectrometer (Optical Resolution 1.5nm, Ocean Optics, Dunedin, FL). This liner CCD-array detector with 2048-element pixels was used for simultaneous detection of the spectrum from 200 to 1100 nm. A note book computer was connected with the spectrometer through a USB cable for display and data processing. All the experiments were performed at room temperature and atmospheric pressure.

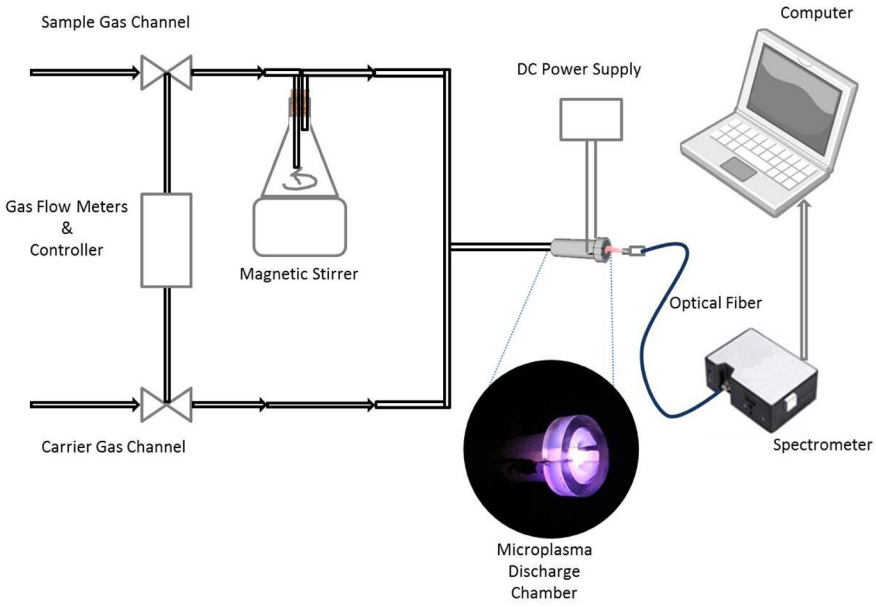

Fig.3 Schematic diagram of the measurement system.

3 Results and discussion

3.1 Microplasma Discharge Characteristics

The discharge characteristics of the microplasma device was studied and reported in our previous paper.[22] A DC voltage was applied to the microplasma device through a power resistor. The argon plasma was generated at atmospheric pressure. The current-voltage characteristics of the microplasma device were measured within the discharge current from 0.28 to 18 mA. The threshold discharge voltage of the microplasma device is 420 V. The discharge voltage varied nonlinearly from 420 to 230 V when the discharge increased from 0.3 to 17.7 mA. Thus the typical discharge parameters for trace gas analysis used in our study are 8 mA and 280 V under the carrier gas flow rate of 1000 mL min^{-1}, where the microplasma emission intensities are stable for experiment.

3.2 Spectroscopy

Since the plasma have high excitation and ionization potentials and generate highly energized metastable species, the microplasma source can provide sufficient energy to fragment and excite targeted nerve agent through Penning ionization with metastable Ar. The metastable Ar generated from the glow discharge plasma impacted with TEP molecules and energy finally passed on to TEP. During these processes, TEP molecules can be broken into small pieces such as elements, organic radicals, and some other parts. The excited species will release particular emissions during returning process to ground states, and therefore, we can use

spectrometer to measure specific spectral lines/bands to identify particular components, elemental, molecular, or radical.

Prior to introducing the sample, the background emission spectrum of the atmospheric pressure argon plasma was recorded in the wavelength region between 200 and 480 nm as shown in Fig. 4. The plasma discharge operated at 8 mA, 280 V, and argon flow rate of 1000 mL min^{-1}. In our interested wavelength region, the spectrum shows typical argon emission lines and significant molecular bands of OH, NH, N_2, and N_2^+ due to the presence of impurities such as air and water.[23] It is known that phosphorus element has two strong emission lines in our measurement range at 213.6 nm and 253.6 nm. From the background spectrum, we can not find any obvious background emission peaks at the vicinity of 213.6 nm and 253.6 nm wavelengths to interfere the detections of phosphorus in nerve agents.

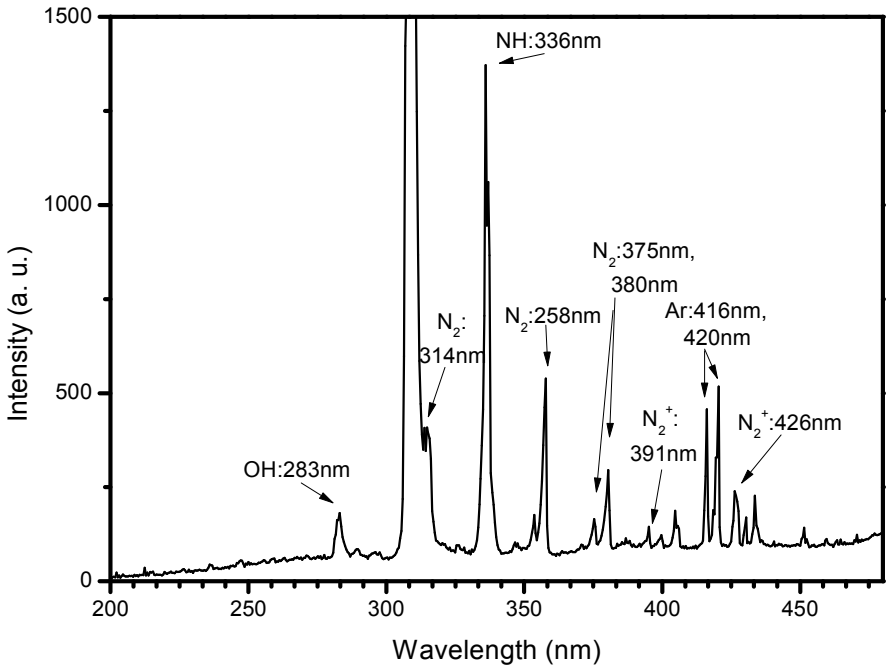

Fig.4 Background of Ar plasma emission spectrum: discharge current, 8 mA; discharge voltage, 280 V; and carrier gas flow rate, 1000 mL min^{-1}.

The TEP vapor was generated from a stirred sealed flask by a magnetic stirrer. The vapor pressure of TEP at 20 ºC is 1 mm Hg .[24] From the ideal gas equation:

$$P = nRT/V \qquad (1)$$

the corresponding concentration of saturated TEP vapor was calculated to be 1125 ppm by volume in an ideal case with adequate stirring. Fig. 5 shows an emission spectrum of 276 ppm TEP in argon plasma under the same discharge condition as that of background. Besides the background peaks, there are also emission peaks of phosphorus at 213.6 nm, 214.9 nm, 253.6 nm, and 255.3 nm. The two strong peaks at 253.6 nm and 213.6 nm were marked in Fig. 5. Because the emission peak at 253.6 nm has the strongest intensity, we used this peak to calibrate the concentration of TEP. Meanwhile, there is a strong emission peak of CH at 431.2 nm. In order to zoom out these peaks, an x axis break from 270 nm to 420 nm was inserted. In order to study the emission spectrum patterns of different plasma-based techniques, a microwave plasma source was employed to substitute the microplasma for comparison. The structure of microwave plasma has been introduced in the experiment section. When argon carried the TEP and flowed through the microwave cavity, microwave plasma was generated. The microwave plasma emission spectrum was recorded as shown in Fig. 6. Comparing the microwave plasma emission spectrum with the microplasma emission spectrum, it was found that both plasma sources had strong emission peaks of phosphorus at 253.6 nm and 213.6 nm, but the emission peak of CH at 431.2 nm almost could not be identified for microwave plasma. It is known that the electrons in DC microplasma and microwave plasma have very high temperatures in the order of 20000 K[25] to fragment and excite targeted nerve agent through Penning ionization and energy transfer. Therefore, the spectra of both plasma sources have emission peaks of phosphorus. However, the gas temperatures of two plasma sources are quite different. The gas temperature of microwave plasma is typically approximately 3000 K.[26] In a general manner, the alkyl phosphates are not thermally stable compounds. When temperature rises to about 200 °C, TEP start to split into CH_4, CO, C_2H_4, C_2H_6, and others without H_2.[27] With the temperature keeps increasing, TEP and the degraded products splits further and generates H_2. When the temperature goes to 1000 °C, 72% H in TEP decomposes and exists in the form of H_2.[28] It is quite reasonable to presume that most of the H in TEP splits out and produces H_2 at the temperature of about 3000 K, which is a typical gas temperature of microwave plasma. Therefore, we can not observe the emission peak of CH at 431.2 nm in the emission spectrum of microwave plasma. However, the gas temperature of a DC microplasma source is much lower compared with a microwave plasma source. Eijkel *et al.*[29] reported that the gas temperature of their microplasma is about 125 °C. The gas temperature of our microplasma source was measured to be about 80 °C using a thermocouple thermometer. In this case, TEP has no thermal decomposition or split.[27] The entire H atoms bond with C. With the excitation of plasma, TEP can emit a peak of CH at 431.2 nm. So the

microplasma we used here is a very unique tool for nerve agent detection through measuring two parts of OP, phosphorus emission and CH emission simultaneously.

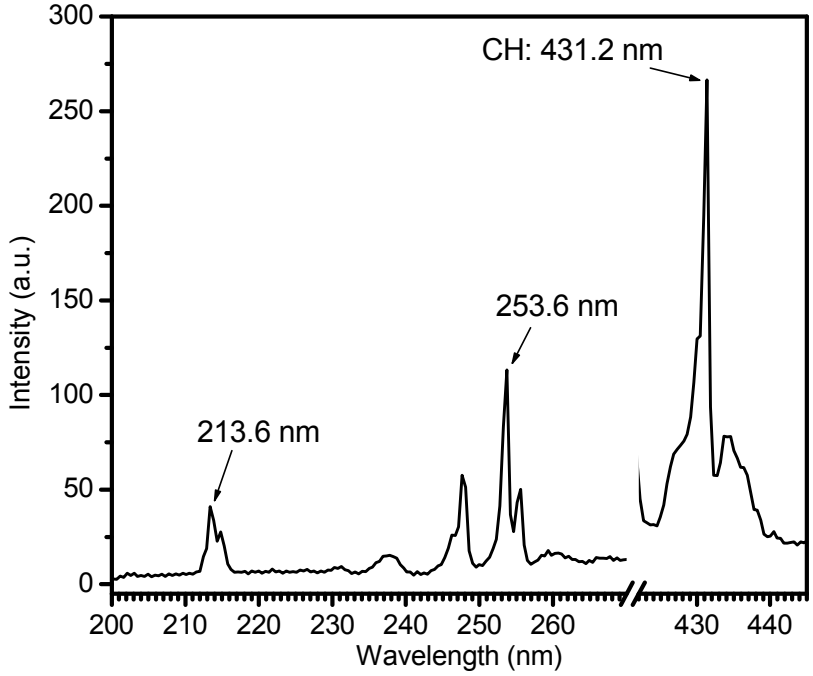

Fig.5 Microplasma emission spectrum of TEP: concentration of TEP, 276 ppm; discharge current, 8 mA; discharge voltage, 280 V; and carrier gas flow rate, 1000 mL min^{-1}.

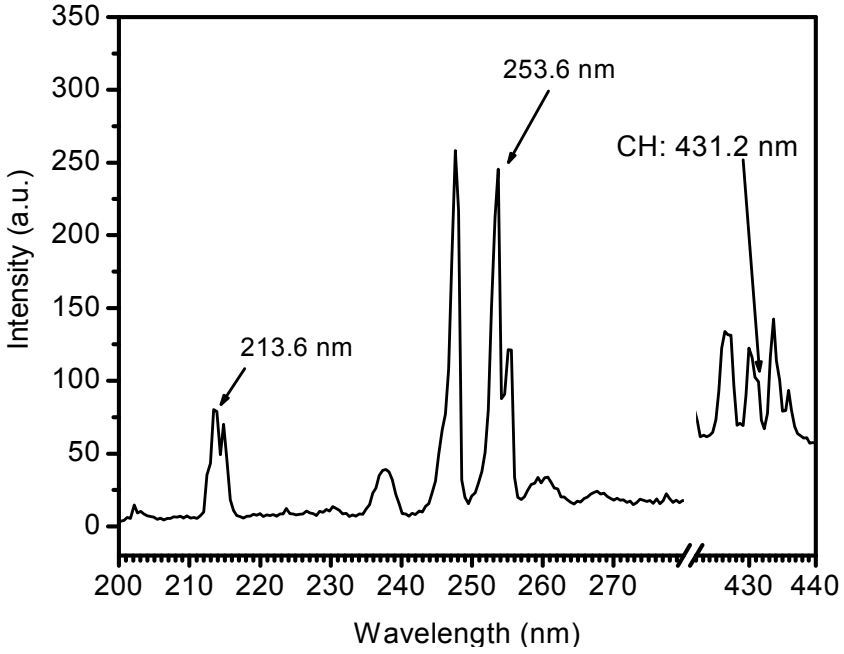

Fig.6 Microwave plasma emission spectrum of TEP: concentration of TEP, 276 ppm; microwave frequency, 2.45 GHz; microwave power, 100 W.

3.3 Influence of operational parameters

The influence of discharge current and gas flow rate on phosphorus signal intensity has been investigated.

In order to investigate the relationship between the emission intensity and the discharge current, we maintained the gas flow rates at 1000 mL min^{-1} and 233.5 mL min^{-1} in carrier gas channel and sample gas channel, respectively. The concentration of TEP is 232 ppm. Because TEP molecule has one phosphorus atom; phosphorus has the same mole concentration with TEP. The discharge current we tested is under 11 mA. When the discharge current gets higher than 11 mA, the discharge status transferred from glow discharge to arc discharge, which is not proper to be employed as an emission source.[22] As shown in Fig. 7, the emission intensity of phosphorus increases linearly with the discharge current in our tested range.

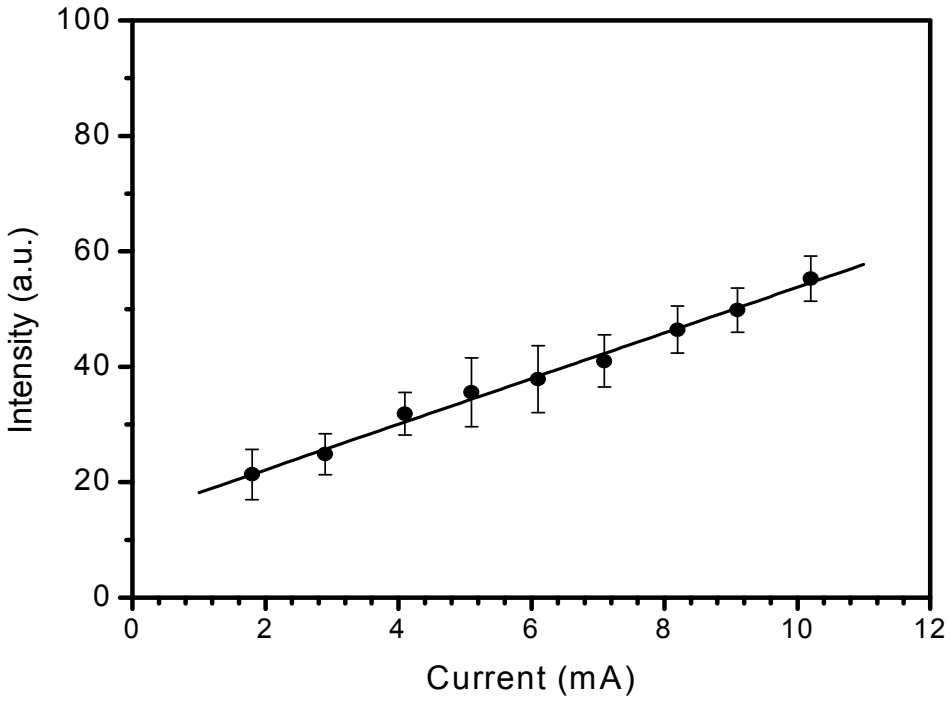

Fig.7 Effect of discharge current on emission intensity of phosphorus at 253.6 nm: concentration of TEP, 232 ppm; carrier gas flow rate, 1000 mL min^{-1}; and sample gas flow rate, 233.5 mL min^{-1}.

The plasma gas flow rate has a significant influence on the emission intensity as shown in Fig. 8. In order that the vapor of TEP is saturated, we tested the total gas flow rate in a range from 275 to 1233.5 mL min^{-1}. The concentration of TEP was kept constant since the sample gas flow rate kept at 233.5 mL min^{-1} invariant when the gas flow rate varied. When the carrier gas flow rate increases, the total molar quantity of TEP linearly increases and results in higher emission intensity. Furthermore, the shape of plasma flame

changes with the gas flow rate. We observed that plasma flame gradually elongated when the gas flow rate increased beyond 750 mL min^{-1}. Meanwhile, the discharge current also slightly increased from 8.0 to 8.2 mA. From the phenomena of views, changes of plasma flame shape and of discharge current may be part of the reasons that cause the nonlinearity between the signal intensity and the flow rate since there are a lot of reasons for this phenomenon.

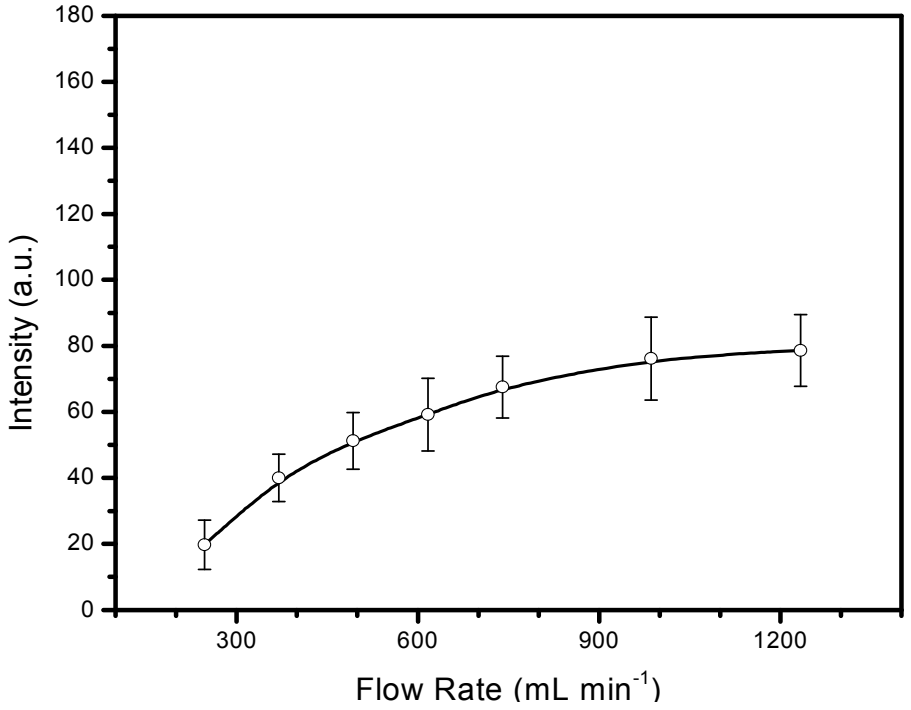

Fig.8 Effect of gas flow rate on emission intensity of TEP at 253.6 nm: concentration of TEP, 232 ppm; discharge current, 8 mA; discharge voltage, 280 V.

3.4 Calibration

The plasma emission intensities of P at 253.6 nm with different concentrations of TEP were measured and calibrated using peak height.1225 ppm saturated TEP vapor was generated in a sealed flask by using a magnetic stirrer and fed into the discharge chamber. The concentration of TEP in the discharge chamber was controlled by adjusting the flow rates of sample and carrier gases. The discharge parameters used for the calibration are 8 mA, 280 V, and 1000 mL min^{-1}. The calibration curve of emission intensity of phosphorus versus the concentration of TEP is shown as the solid line in Fig. 9. In order to obtain a high concentration of TEP, the gas flow rate in sample gas channel has to increase. It may also result in unsaturation of TEP vapor. Therefore, the calibration range is limited to about 500 ppm.

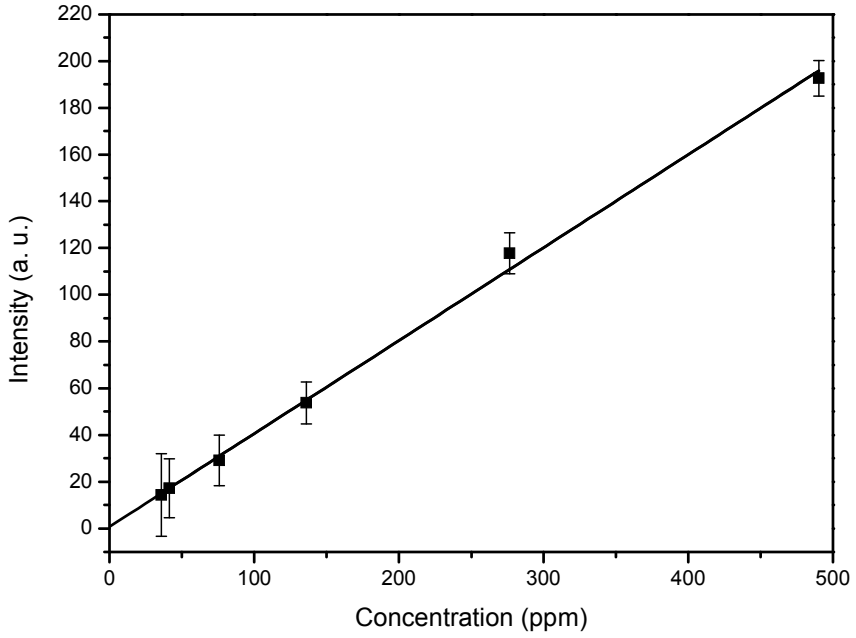

Fig.9 Calibration curves of TEP detection: discharge current, 8 mA; discharge voltage, 280 V; and carrier gas flow rate, 1000 mL min^{-1}.

3.5 Analytical Performance

Due to the dilution capability of our mass flow controllers, the lowest obtainable concentration of TEP in this experimental set up is 41 ppm. Concentration lower than 41 ppm was not measured in this study. The emission peak of 41 ppm TEP was recorded and shown in Fig. 10. In our previous study, the detection limit of this device for hydrocarbons was as low as ppb level[21]. Based on the relative standard deviation of the background and signal, we calculated the detection limits of TEP with our microplasma-based detector to be about 5 ppm.[22]

To investigate the stability of our microplasma, TEP vapor with a concentration of 276 ppm was carried by argon into the discharge chamber at a flow rate of 1000 mL min^{-1}. The plasma device was continuously operated for 105 minutes at 8 mA. The emission intensity of phosphorus at 253.6 nm and the base line intensity at 228.7 nm were recorded in Fig. 11. It was found that the microplasma stably operated during the experiment. The standard deviation of these intensities at 253.6 nm and 228.7 nm are ±0.74 and ±0.32 a. u., respectively. As mentioned above, the low gas temperature (~80 °C) is characteristic of our microplasma source. Owing to this unique property, our microplasma device overcomes the problem of carbon deposition,

which is very common for the hydrocarbon detection using plasma-based detectors.[22] Therefore, such improved stability was achieved for our microplasma device.

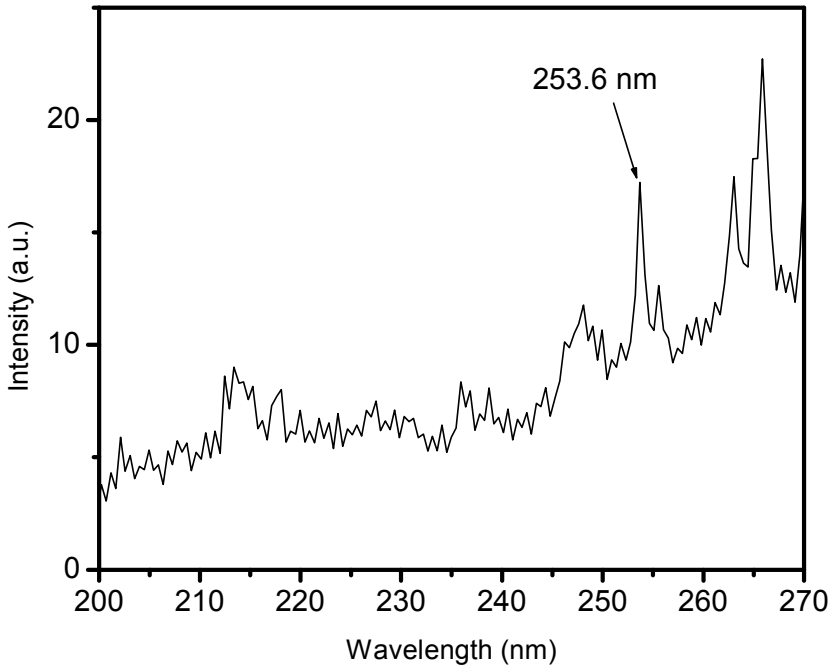

Fig.10 Emission spectrum of TEP at a concentration of 41 ppm: discharge current, 8 mA; discharge voltage, 280 V; and gas flow rate, 1000 mL min^{-1}.

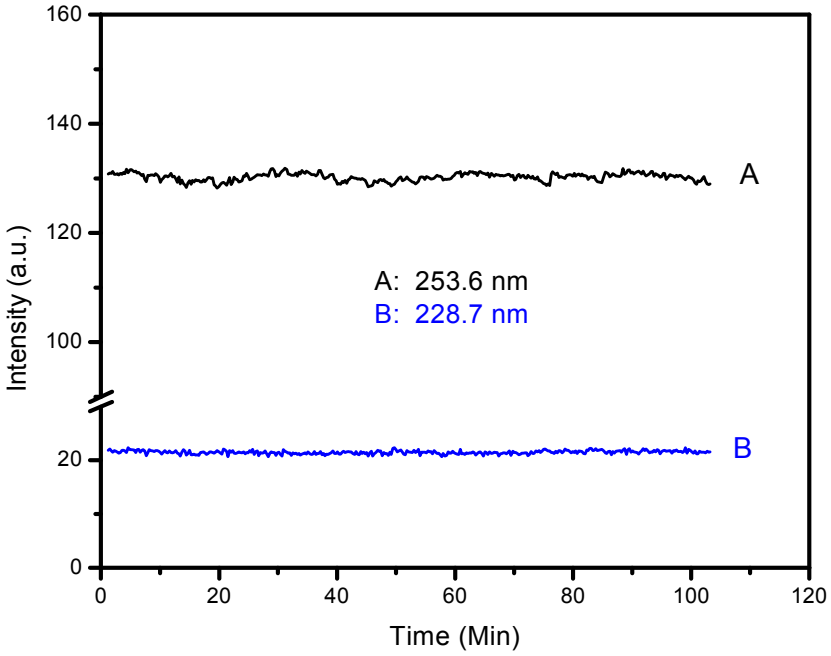

Fig.11 Stability of plasma source: concentration of TEP, 276 ppm; discharge current, 8 mA; discharge voltage, 280 V; and gas flow rate, 1000 mL min^{-1}.

4 Conclusions

This study suggests that our direct current glow discharge microplasma combined with spectrometer could be a significant tool in the field of nerve agents scanning. From a security point of view, TEP was chosen as a representative nerve agent in this experiment and the detection limit of it was calculated to be 5 ppm by volume which can meet the actual needs. Advantages of our method over typically used flame photometry technology include detect two parts of the nerve agent components, phosphorous element and organic part of CH radicals at the same time which enhances the selectivity to nerve agents. In addition, the comparison of different plasma based device such as microwave plasma imply that the very low gas temperature of our microplasma source makes it unique to simultaneously detect phosphorous element and organic part of CH radicals since there is no thermal decomposition or split of TEP molecules. Based on the same mechanism, our microplasma device can simultaneously detect sulfur and CH radical as well. Therefore, the technique can be extended to screening sulfur-containing chemical warfare agents, like mustard, sesquimustard, and thiodiglycol. Thus because of the small size, light weight, and low power, our microplasma device will be a very good candidate of a portable instrument for chemical warfare agents scanning with miniature power supply and spectrometer in the future.

Acknowledgements

The authors are grateful for financial support from National Recruitment Program of Global Experts (NRPGE), the Hundred Talents Program of Sichuan Province (HTPSP), and the Startup Funding of Sichuan University for setting up the Research Center of Analytical Instrumentation.

References

1. E. W. J. Hooijschuur, C. E. Kientz, U. A. T. Brinkman, *Journal of Chromatography A*, 2002, **98**, 277-200.
2. M. Pumera, *Journal of Chromatography A*, 2006, **1113**, 5-13.
3. http://en.wikipedia.org/wiki/Nerve_agent, 2006 (accessed 29. 12. 06).
4. S. S. Brody, J. E. Chaney, *Journal of Gas Chromatography*, 1966, **4**, 42-46.
5. H. C. Trap, J. P. Langenberg, *Journal of High Resolution Chromatography*, 1999, **22**, 153-158.
6. A. Kaipainen, O. Kostiainen, M. L. Riekkola, *Journal of Microcolumn Separations*, 1992, **4**, 245-251.
7. D. J. McGarvey, J. R. Stuff, B. R. Williams, H. D. Durst, *Spectroscopy Letters*, 2000, **33**, 795-819.
8. M. T. Soderstrom, R. A. Ketola, O. Kostiainen, *Fresenius' Journal of Analytical Chemistry*, 1995, **352**, 550-556.
9. H. D. Durst, J. R. Mays, J. L. Ruth, B. R. Williams, R. V. Duevel, *Analytical Letters*, 1998, **311**, 429-1444.
10. A. A. Tomchenko, G. P. Harmer, B. T. Marquis, *Sensors and Actuators B*, 2005, **108**, 41-55.
11. J. P. Novak, E. S. Snow, E. J. Houser, D. Park, J. L. Stepnowski, R. A. McGill, *Applied Physics Letters*, 2003, **83**, 4026-4028.
12. G. R. Asbury, C. Wu, W. F. Siems, H. H. Hill, *Analytica Chimica Acta*, 2000, **404**, 273-283.
13. J. D. Skalny, J. Orszagh, N. J. Mason, J. A. Rees, Y. Aranda-Gonzalvo, T. D. Whitmore, *Int. J. Mass Spectrom.*, 2008, **272**, 12−21.
14. S. Yasuo, K. Mieko, T. Koichiro, O. Isaac, I. Kazumitsu, I. Teruo, S. Hiroyuki, M. Koji, Y. Shigeharu, S. Yasuhiro, S. Hiroshi, M. Hisashi, T. Yasuo, S. Ryoji, O. Akihiko, T. Yasuaki, N. Hisashi, W. Izumi, E. Naoya, T. Hiroyuki, H. Shigeru, F. Masumi, O. Hidehiro, *Analytical Chemistry*, 2013, **85**, 2659-2666.
15. R. B. Cody, J. A. Larame´ e, H. D. Durst, *Analytical Chemistry*, 2005, **77**, 2297–2302.
16. J. M. Nilles, T. R. Connell, H. D. Durst, *Analytical Chemistry*, 2009, **8**, 16744–6749.
17. W. Lindinger, H. A. Jordan, *Int. J. Mass Spectrom. Ion Process*, 1998, **173**, 191 −241.
18. R. S. Blake, C. Whyte, C. O. Hughes, A. M. Ellis, P. S. Monks, *Analytical Chemistry*, 2004, **76**, 3841−3845.
19. X. Yuan, X. L. Ding, Z. J. Zhao, X. F. Zhan, Y. X. Duan, *J. Anal. At. Spectrom.*, 2012, **27**, 2094–2101.
20. X. L. Ding, X. F. Zhan, X. Yuan, Z. J. Zhao, Y. X. Duan, *Analytical Chemistry*, 2013, **85**, 9013-9020.

21. Y. X. Duan, Y. X. Su, Z. Jin, *Review of Scientific Instruments*, 2003, **74**, 2811-2816.

22. Y. Liu, W. Q. Cao, X. L. Ding, X. Yuan, Y. X. Duan, *Spectrochimica Acta Part B* , 2012, **76**, 152-158.

23. Z. Jin, Y, Su, Y. X. Duan, *Analytical Chemistry*, 2001, **73**, 360-365.

24. Material Safety Data Sheet, https://fscimage.fishersci.com/msds/14338.htm, 2007 (accessed 08. 01 2007).

25. J. Jonkers, L. J. M. Selen, J.A. M. van der Mulleny, E. A. H. Timmermans, D. C. Schram, *Plasma Sources, Science and Technology*, 1997, **6**, 533-539.

26. A. Bogaerts, E. Neyts, R. Gijbels, van der Mullen, *J. Spectrochimica Acta - Part B Atomic Spectroscopy*, 2002, **57**, 609-658.

27. C. E. Higgins, W. H. Baldwin, *Journal of Organic Chemistry*, 1965, **30**, 3173-3176.

28. V. Lhomme, C. Bruneau, N. Soyer, A. Brault, *Industrial & Engineering Chemistry Product Research and Development*, 1984, **23**, 98-102.

29. J. C. T. Eijkel, H. Stoeri, A. Manz, *Analytical Chemistry*, 2002, **72**, 2547-2552.

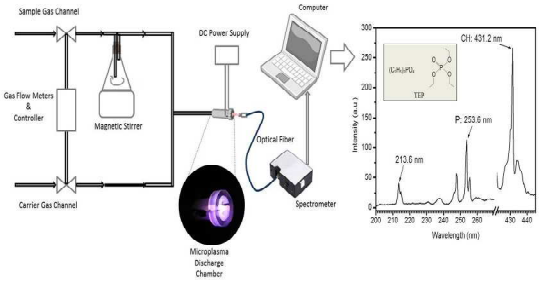

A newly designed microplasma device can detect two parts of the nerve agent components simultaneously which enhances the selectivity in analysis.